

# Synthesis and Characterization of Os and Pt–Os/Carbon Nanocomposites and their Relative Performance as Methanol Electrooxidation Catalysts

Joshua T. Moore,<sup>†</sup> Deryn Chu,<sup>‡</sup> Rongzhong Jiang,<sup>‡</sup> Gregg A. Deluga,<sup>§</sup> and C. M. Lukehart<sup>\*,†</sup>

Department of Chemistry, Vanderbilt University, Nashville, Tennessee 37235, Electrochemistry Branch, Sensors and Electron Devices Directorate, U.S. Army Research Laboratory, Adelphi, Maryland 20783-1197, and Corrosion Research Center, Department of Chemical Engineering and Materials Science, University of Minnesota, Minneapolis, Minnesota 55455

Received November 12, 2001. Revised Manuscript Received December 23, 2002

Thermal treatment of *cis*-(2,2'-bipyridine)<sub>2</sub>OsCl<sub>2</sub>, (η<sup>6</sup>-cymene)<sub>2</sub>Os<sub>2</sub>Cl<sub>4</sub>, or [(bpy)<sub>2</sub>Os(μ-bpm)-PtCl<sub>2</sub>][CF<sub>3</sub>SO<sub>3</sub>]<sub>2</sub>/Vulcan carbon powder composites under solely reductive conditions affords Os or Pt–Os/carbon nanocomposites consisting of metal nanoparticles highly dispersed on the carbon support. Nanocomposites containing ca. 35–50 wt % metal with metal nanocrystals of ca. 5–6 nm average diameter are formed. Evaluation of the performance of these nanocomposites as methanol electrooxidation catalysts in direct methanol fuel cells and in an electrochemical cell designed for combinatorial testing reveals that, although the Os/carbon nanocomposites and the Pt–Os alloy/carbon nanocomposite give open circuit potentials indicative of thermodynamically favorable methanol oxidation, the kinetics of these oxidations are too low to be of practical importance. Unfortunately, the Os-containing electrocatalysts prepared by this synthesis strategy did not exhibit high performance for methanol oxidations as predicted by theoretical computations.

## Introduction

In direct-methanol fuel cells (DMFCs), aqueous methanol is electrooxidized to produce CO<sub>2</sub> and electrical current.<sup>1</sup> Electrocatalysts having higher activity for methanol oxidation are critically needed to enhance DMFC performance for commercial device applications. Such catalysts are usually prepared as unsupported metal colloids or as nanocomposites in which metal nanoparticles are supported on an electrically conducting carbon of high surface area. The search for active methanol oxidation catalysts has involved extensive variation of catalyst composition and mode of catalyst preparation.

Mixed-metal colloids or nanocomposites containing Pt along with one or more less noble metals are currently favored as methanol electrooxidation catalysts.<sup>1,2</sup> A bifunctional reaction mechanism is usually invoked to explain the contribution of each metal to the overall reaction. Pt activates C–H bond cleavage within surface-adsorbed methanol molecules producing a Pt<sub>x</sub>–CO surface species, whereas an oxophilic metal activates adsorbed water to accelerate oxidation of surface-adsorbed CO to CO<sub>2</sub>. The absence of an oxophilic metal usually leads to CO poisoning of the anode catalyst in working DMFCs.

Computational results reported recently by Kua and Goddard<sup>3</sup> for the stepwise oxidation of methanol by several Group VIII transition metals support a bifunctional mechanism for methanol oxidation by conventional Pt–Ru catalysts. In addition, this theoretical analysis also reveals the unexpected result that Os metal should activate both methanol and water sufficiently well to serve as a mono-metallic methanol oxidation catalyst, and an invitation for experimental verification of this prediction has been extended. Although there have been several reports of methanol oxidation using Pt–Os alloys,<sup>2,4</sup> to our knowledge no one

\* Author to whom correspondence should be addressed. Phone: 615-322-2935. Fax: 615-322-4936. E-mail: charles.m.lukehart@vanderbilt.edu.

<sup>†</sup> Vanderbilt University.

<sup>‡</sup> U.S. Army Research Laboratory.

<sup>§</sup> University of Minnesota.

(1) (a) Hammett, A. *Catal. Today* **1997**, *38*, 445. (b) Hogarth, M. P.; Hards, G. A. *Platinum Met. Rev.* **1996**, *40*, 150. (c) Chandler, G. K.; Genders, J. D.; Pletcher, D. *Platinum Met. Rev.* **1997**, *41*, 54. (d) Ralph, T. R. *Platinum Met. Rev.* **1997**, *41*, 102. (e) Hammett, A.; Troughton, G. L. *Chem. Ind.* **1992**, 480. (f) Ren, X.; Wilson, M. S.; Gottesfeld, S. *J. Electrochem. Soc.* **1996**, *143*, L12. (g) Hogarth, M. P.; Christensen, P. A.; Hammett, A. *Proc. First Int. Symp. New Mater. Fuel Cells* **1995**, 310. (h) Lin, W. F.; Wang, J. T.; Savinell, R. F. *J. Electrochem. Soc.* **1997**, *144*, 1917. (i) Gasteiger, H. A.; Markovic, N.; Ross, P. N., Jr.; Cairns, E. J. *J. Electrochem. Soc.* **1994**, *141*, 1795. (j) Surampudi, S.; Narayanan, S. R.; Vamos, E.; Frank, H.; Halpert, G.; LaConti, A.; Kosek, J.; Surya Prakash, G. K.; Olah, G. A. *J. Power Sources* **1994**, *47*, 377. (k) Wang, K.; Gasteiger, H. A.; Markovic, N. M.; Ross, P. N., Jr. *Electrochim. Acta* **1996**, *41*, 2587. (l) Pathanjali, G. A.; Krishnamurthy, B.; Chireau, R. F.; Mital, C. K. *Bull. Electrochem.* **1996**, *12*, 193.

(2) (a) Reddington, E.; Sapienza, A.; Gurau, B.; Viswanathan, R.; Saragapani, S.; Smotkin, E. S.; Mallouk, T. E. *Science* **1998**, *280*, 1735. (b) Gurau, B.; Viswanathan, R.; Liu, R.; Lafrenz, T.; Lye, K. L.; Smotkin, E. S.; Reddington, E.; Sapienza, A.; Chan, B. C.; Mallouk, T. E.; Saragapani, S. *J. Phys. Chem. B* **1998**, *102*, 9997. (c) Gotz, M.; Wendt, H. *Electrochim. Acta* **1998**, *43*, 3637.

(3) Kua, J.; Goddard, W. A. *J. Am. Chem. Soc.* **1999**, *121* (47), 10928–10941.

has examined Os as an electrocatalyst in working DMFCs.

As part of an ongoing investigation to prepare metal alloy/carbon nanocomposites exhibiting high performance as DMFC anode catalysts,<sup>5</sup> we now report the synthesis and characterization of two Os/Vulcan carbon powder nanocomposites along with a determination of the relative performance of these nanocomposites as methanol electrooxidation catalysts. These nanocomposites are prepared using either organometallic or nonorganometallic molecular precursors as sources of Os metal. Each nanocomposite is prepared at high metal loading while maintaining acceptably small Os nanocrystals to provide a good test of DMFC relative performance.<sup>5</sup> Although both Os/carbon nanocomposites give open circuit potentials indicative of thermodynamically favorable methanol oxidation, the rate of this oxidation is, unfortunately, too slow to be of practical importance.

To potentially improve the methanol oxidation performance of these Os-containing nanocomposites through a bifunctional catalyst mechanism, elemental Pt was introduced as a second metal component. Physical mixtures of each Os/carbon nanocomposite with Pt black were prepared and tested electrochemically for methanol oxidation. In addition, a Pt–Os alloy/carbon nanocomposite was prepared using a 1:1 Pt–Os bimetallic precursor as the source of metal and was tested under identical conditions. Although inclusion of Pt metal as either a compounding additive or as an alloying element improves the thermodynamics of methanol electrooxidation, the kinetics of this reaction remains significantly less than that observed for conventional Pt–Ru catalysts.

## Experimental Section

**General Methods.** The two precursor complexes used as sources of Os, *cis*-(2,2'-bipyridine)<sub>2</sub>OsCl<sub>2</sub>, **1a**, [*cis*-(bpy)<sub>2</sub>OsCl<sub>2</sub>]<sup>6</sup> and (η<sup>6</sup>-1-isopropyl, 4-methylbenzene)<sub>2</sub>Os<sub>2</sub>Cl<sub>4</sub>, **2b**, [(η<sup>6</sup>-cymene)<sub>2</sub>Os<sub>2</sub>Cl<sub>4</sub>],<sup>7</sup> and the reagent, *cis*-(dimethyl sulfoxide)<sub>2</sub>PtCl<sub>2</sub>,<sup>8</sup> were prepared according to literature procedures. Successful precursor preparation was confirmed using high-field <sup>1</sup>H NMR spectroscopy. 2,2'-Bipyrimidine was purchased from Lancaster chemicals and was used as received. All solvents were reagent grade and were used as received. Vulcan carbon powder XC-72R was obtained commercially from Cabot Corporation.

(4) (a) Crown, A.; Kim, H.; Lu, G. Q.; de Moraes, I. R.; Rice, C.; Wieckowski, A. *J. New Mater. Electrochem. Syst.* **2000**, *3*, 275. (b) Reddington, E.; Yu, J. S.; Sapienza, A.; Chan, B. C.; Gurau, B.; Viswanathan, R.; Liu, R.; Smotkin, E. S.; Sarangapani, S.; Mallouk, T. E. *Mater. Res. Soc. Symp. Proc.* **1999**, *549*, 231. (c) Liu, R.; Let, K. L.; Pu, C.; Fan, Q.; Leyarovsky, N.; Segre, C.; Smotkin, E. S. *Proc. Electrochem. Soc.* **1996**, *96* (8), 341. (d) Hamnett, A.; Kennedy, B. J. *Electrochim. Acta* **1988**, *33*, 1613.

(5) (a) Steigerwalt, E. S.; Deluga, G. A.; Lukehart, C. M. *J. Phys. Chem. B* **2002**, *106*, 760. (b) Steigerwalt, E. S.; Deluga, G. A.; Cliffl, D. E.; Lukehart, C. M. *J. Phys. Chem. B* **2001**, *105*, 8097. (c) Boxall, D. L.; Deluga, G. A.; Kenik, E. A.; King, W. D.; Lukehart, C. M. *Chem. Mater.* **2001**, *13*, 891. (d) Lukehart, C. M.; Boxall, D. L.; Corn, J. D.; Hariharasarma, M.; King, W. D.; Kwiatkowski, K. C.; Steigerwalt, E. S.; Kenik, E. A. *ACS Fuel Chem. Div. Preprints* **1999**, *44*, (4), 982. (e) Boxall, D. L.; Lukehart, C. M.; Kenik, E. A. *Proc. ASME Adv. Energy Syst. Div.* **1999**, *39*, 327. (f) Boxall, D. L.; Kenik, E. A.; Lukehart, C. M. *Mater. Res. Soc. Symp. Proc.* **2001**, *589*, 265. (g) Lukehart, C. M. U.S. Patent 6,232,264, May 15, 2001.

(6) Buckingham, D. A.; Dwyer, F. P.; Goodwin, H. A.; Sargeson, A. M. *Aust. J. Chem.* **1964**, *17*, 325.

(7) Cabeza, J. A.; Maitlis, P. M. *J. Chem. Soc. Dalton Trans.* **1985**, 573.

(8) Price, J. H.; Williamson, A. N.; Schramm, R. F.; Wayland, B. B. *Inorg. Chem.* **1972**, *11*, 1280.

Microanalyses were performed by Galbraith Laboratories, Inc., Knoxville, TN, or by Atlantic Microlab, Inc., Norcross, GA. Os content could not be obtained by commercial microanalysis because of its toxicity and the high volatility of Os oxides. Metal content of the nanocomposite materials was estimated from sample weight gain measurements for the Os nanocomposites (**1b**, 48 wt % Os; **2b**, 47 wt % Os) or from Pt analysis and EDS spectral data for the Pt–Os nanocomposite **3b** (35 wt % total metal). The following abbreviations are used: bpy = 2,2'-bipyridine, C<sub>10</sub>H<sub>8</sub>N<sub>2</sub>; bpm = 2,2'-bipyrimidine, C<sub>8</sub>H<sub>6</sub>N<sub>4</sub>; DMSO = (CH<sub>3</sub>)<sub>2</sub>SO.

Samples for transmission electron microscopy (TEM) imaging were prepared by placing a drop of nanocomposite/CH<sub>2</sub>Cl<sub>2</sub> suspension onto a 3-mm diameter copper grid coated with holey carbon, followed by evaporation of the solvent. Particle-size distributions for nanocomposite materials were obtained by measuring particle diameters directly from bright-field micrographs recorded on a Philips CM20T TEM operating at 200 kV.

X-ray diffraction (XRD) scans were obtained using a Scintag X1 θ/θ automated powder X-ray diffractometer with a Cu target, a Peltier-cooled solid-state detector, and a zero-background, Si(510) sample support. For particle-size determinations, each XRD scan was corrected for background scattering and was stripped of the K<sub>α2</sub> portion of the diffracted intensity using the DMSNT software (version 1.30c) provided by Scintag. Observed peaks were fitted with a profile function to extract the full-width-at-half-maximum (fwhm) values. Average crystallite size, *L*, was calculated from Scherrer's equation assuming that peak broadening arises from size effects only.<sup>9</sup>

**Preparation of [(bpy)<sub>2</sub>Os(bpm)](CF<sub>3</sub>SO<sub>3</sub>)<sub>2</sub>·2H<sub>2</sub>O.** The complex [(bpy)<sub>2</sub>Os(bpm)](CF<sub>3</sub>SO<sub>3</sub>)<sub>2</sub>·2H<sub>2</sub>O was prepared using a variation of the procedure published by Goldsby and Meyer for the preparation of the corresponding hexafluorophosphate salt.<sup>10</sup> A solution of 0.198 g of (bpy)<sub>2</sub>OsCl<sub>2</sub> and 0.093 g of bpm were refluxed in 40 mL of 2:1 ethanol/water solvent for 36 h under a N<sub>2</sub> atmosphere. After this time, a 3-fold excess of AgOTf (0.267 g) was added to the reaction solution to effect anion exchange, and the solution was refluxed for an additional 2 h. Upon cooling to room temperature, the resulting AgCl precipitate was removed by filtration through a pad of Celite diamotaceous earth on a medium ceramic frit, and the filtrate was evaporated to dryness at reduced pressure. The reaction residue was dissolved in a minimum volume of absolute ethanol and was flash-precipitated by addition of anhydrous diethyl ether. Purification was carried out by separation on a 4 × 15 cm alumina (80–200 mesh; Fisher Scientific) column using acetonitrile as the mobile phase. The desired product was eluted first as a dark purple band. The appropriate fraction was collected and was concentrated at reduced pressure. The product complex was precipitated from solution by addition of diethyl ether, isolated by filtration, and dried at reduced pressure (70% yield). Anal. Calcd for [(C<sub>10</sub>H<sub>8</sub>N<sub>2</sub>)<sub>2</sub>Os(C<sub>8</sub>H<sub>6</sub>N<sub>4</sub>)](CF<sub>3</sub>SO<sub>3</sub>)<sub>2</sub>·2H<sub>2</sub>O: C, 44.77; H, 3.26; N, 13.93. Found: C, 44.25; H, 3.10; N, 13.14.

**Preparation of [(bpy)<sub>2</sub>Os(μ-bpm)PtCl<sub>2</sub>](CF<sub>3</sub>SO<sub>3</sub>)<sub>2</sub>·2H<sub>2</sub>O, **3a**.** Complex **3a** was prepared using a variation of the procedure published by Sahai and Rillema for preparation of the related complex [(bpy)<sub>2</sub>Ru(μ-bpm)PtCl<sub>2</sub>](ClO<sub>4</sub>)<sub>2</sub>.<sup>11</sup> A methanol solution of 0.40 g of [(bpy)<sub>2</sub>Os(μ-bpm)](CF<sub>3</sub>SO<sub>3</sub>)<sub>2</sub>·2H<sub>2</sub>O and 0.176 g of (DMSO)<sub>2</sub>PtCl<sub>2</sub> was refluxed in degassed methanol for 12 h in the dark. The resulting solution was evaporated to dryness at reduced pressure. The obtained residue was dissolved in a minimum volume of absolute ethanol, and the crude product was flash-precipitated by addition of anhydrous diethyl ether. Purified product was obtained by repeating the flash precipitation procedure two additional times. Complex **3a** was isolated by filtration and dried at reduced pressure

(9) Klug, H. P.; Alexander, L. E. *X-ray Diffraction Procedures for Polycrystalline and Amorphous Materials*, 2nd ed.; Wiley: New York, 1974.

(10) Goldsby, K. A.; Meyer, T. J. *Inorg. Chem.* **1984**, *23*, 3002.

(11) Sahai, R.; Rillema, D. P. *Inorg. Chim. Acta* **1986**, *118*, L35.

(90% yield). Anal. Calcd for  $[(C_{10}H_8N_2)_2Os(C_8H_6N_4)PtCl_2](CF_3SO_3)_2 \cdot 2H_2O$ : C, 28.57; H, 2.08; N, 8.89. Found: C, 28.00; H, 1.86; N, 8.68.

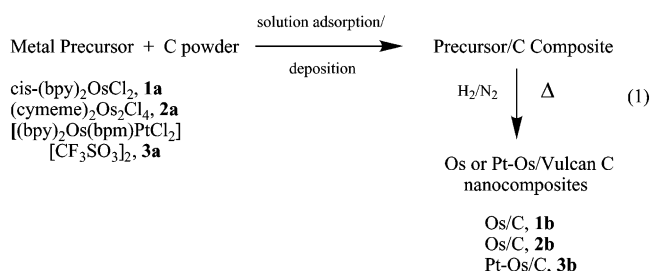
**General Preparation of the Os/Vulcan Carbon Nanocomposites (1b) and (2b).** Nanocomposites **1b** and **2b** were prepared using a two-step deposition/thermal treatment procedure to form Os/carbon nanocomposites of ca. 50 wt % Os metal. Approximately one-half of the required portion of precursor **1a** or **2a** was dissolved in  $CH_2Cl_2$ . To this solution was added the appropriate mass of Vulcan carbon support. The resulting slurry was stirred for 1 h under  $N_2$  to permit adsorption of precursor, and the precursor/carbon composite was isolated as a dry black solid upon removal of residual solvent at reduced pressure. Precursor/carbon composites were placed into a glazed alumina combustion boat, inserted into a Lindberg Blue programmable tube furnace, and heated under a flow (150 mL/min) of getter gas (90:10,  $N_2/H_2$ ) from room temperature to 500 °C at 15 °C/min. For the first thermal treatment, the reaction boat was cooled to room temperature immediately after reaching 500 °C. This procedure was then repeated one additional time to give the desired metal loading. For the second thermal treatment, the reaction boat was held at maximum temperature for 3 h before cooling to ambient temperature under a flow of  $N_2$  gas. Inert or reducing atmospheres were strictly maintained to minimize Os metal oxidation.

**Preparation of the Pt–Os/Vulcan Carbon Nanocomposite, 3b.** A Pt–Os/Vulcan carbon nanocomposite having a total metal loading of ca. 35 wt % was prepared using a two-step deposition/thermal treatment procedure. Approximately one-half of the required amount of precursor **3a** (0.386 g) was dissolved in  $CH_2Cl_2$ . To this solution was added 0.383 g of Vulcan carbon powder. The resulting slurry was stirred for 1 h under  $N_2$  to permit adsorption of precursor, and the precursor/carbon composite was isolated as a dry black solid upon removal of residual solvent at reduced pressure. The precursor/carbon composite was placed into a glazed alumina combustion boat, inserted into a Lindberg Blue programmable tube furnace, and heated under a flow (150 mL/min) of getter gas (90:10,  $N_2/H_2$ ) from room temperature to 500 °C at 15 °C/min. For the first thermal treatment, the reaction boat was cooled to room temperature after heating at 500 °C for 30 min. This procedure was then repeated one additional time to give the desired metal loading. For the second thermal treatment, the reaction boat was held at 500 °C for 3 h before cooling to ambient temperature under a flow of  $N_2$  gas. An inert or reducing atmosphere was strictly maintained to minimize Os metal oxidation. Anal. Found: Pt, 16.77.

**Direct Methanol Fuel Cell and Electrochemical Testing Procedures.** Os/carbon nanocomposites, **1b** and **2b**, and the Pt–Os/Vulcan carbon nanocomposite, **3b**, prepared in this study along with unsupported Pt and  $Pt_1Ru_1$  colloids (Alfa Aesar) were tested as methanol electrooxidation catalysts. For direct methanol fuel cell (DMFC) measurements, detailed procedures for the preparation of membrane electrode assemblies (MEAs) and DMFC testing procedures have been published (U.S. Patent 5599638).<sup>5c</sup> Combinatorial electrochemical measurements were performed using proprietary technology developed at the Army Research Laboratory.<sup>12</sup> For these electrochemical measurements, anode electrodes were spotted on a graphite plane with an exposed surface area of 0.03 cm<sup>2</sup> for each sample tested. The cathode was Pt black having a larger exposed surface area. An electrolyte probe consisting of 3 M  $H_2SO_4$  was used to connect anode and cathode electrodes and form separated methanol fuel cells. The anode fuel was 3 M methanol in 3 M  $H_2SO_4$  under an Ar atmosphere, while the cathode fuel was air. All measurements were recorded at 16 °C.

## Results and Discussion

Complexes **1a**, **2a**, and **3a** are readily soluble in polar organic solvents and can be deposited onto commercial Vulcan carbon powder by adsorption and subsequent solvent evaporation to give precursor/carbon composites of arbitrary loading. Reactive, thermal degradation of these precursor/carbon composites in a partial atmosphere of hydrogen affords Os or Pt–Os/carbon nanocomposites **1b–3b**, as shown in eq 1. Although products of precursor decomposition have not been identified for these syntheses, careful study of the reductive decomposition of a related Pt–Ru precursor complex indicates that organic ligands are volatilized either intact or as hydrogenated species, and chloro ligands are lost as  $HCl$ .<sup>5b,13</sup> A two-step deposition procedure is used to minimize metal particle agglomeration during synthesis. The total metal content of the final Os or Pt–Os/carbon nanocomposites, **1b**, **2b**, and **3b** are 48, 47, and 35 wt %, respectively.



Bright-field TEM micrographs typical of nanocomposites **1b–3b** reveal metal nanoclusters of high contrast dispersed on the amorphous Vulcan carbon powder support (Figure 1). Typical histograms of metal particle diameters are shown in Figure 2. The observed log-normal particle size distribution is consistent with a coalescence growth mechanism of surface-supported metal particles.<sup>14</sup> Average metal nanocluster diameters with standard deviations as determined by TEM are  $6.0 \pm 2.5$  nm for nanocomposite **1b**,  $5.0 \pm 1.5$  nm for nanocomposite **2b**, and  $6.5 \pm 2$  nm for nanocomposite **3b**. EDS spectra collected from broad sample areas, Figure 3, reveal X-ray emission lines expected for Os (nanocomposites **1b** and **1b**) and for both Pt and Os (nanocomposite **3b**). Integrations of EDS peak intensities for resolved Pt and Os emission lines of nanocomposite **3b** gives a Pt/Os stoichiometry of  $Pt_1Os_{1.1}$ . Knowing the Pt loading from bulk elemental analysis, the Os content is calculated to be 18.0 wt % giving a total metal loading of 34.8 wt % for this nanocomposite. Emission from the copper is also observed. X-ray emission from residual chlorine is not observed indicating complete degradation of the molecular precursors within the EDS detection limit.

XRD scans typical of nanocomposites **1b–3b** reveal the expected diffraction patterns (Figure 4). A broad peak centered near 24° in  $2\theta$  is characteristic of amorphous scattering from the Vulcan carbon support. For nanocomposites **1b** and **2b**, all of the remaining peaks of strong intensity have positions and relative intensities expected for diffraction from Os metal. A determi-

(12) (a) Chu, D.; Jiang, R. *Proc.-Electrochem. Soc.* **2001**, C1–86 (Direct Methanol Fuel Cells Electrocatalysis), 188. (b) Patent pending.

(13) Steigerwalt, E. S. Ph.D. Dissertation, Vanderbilt University, Nashville, TN, 2001.

(14) Granqvist, C. G.; Buhrman, R. A. *J. Catal.* **1976**, 42, 477.



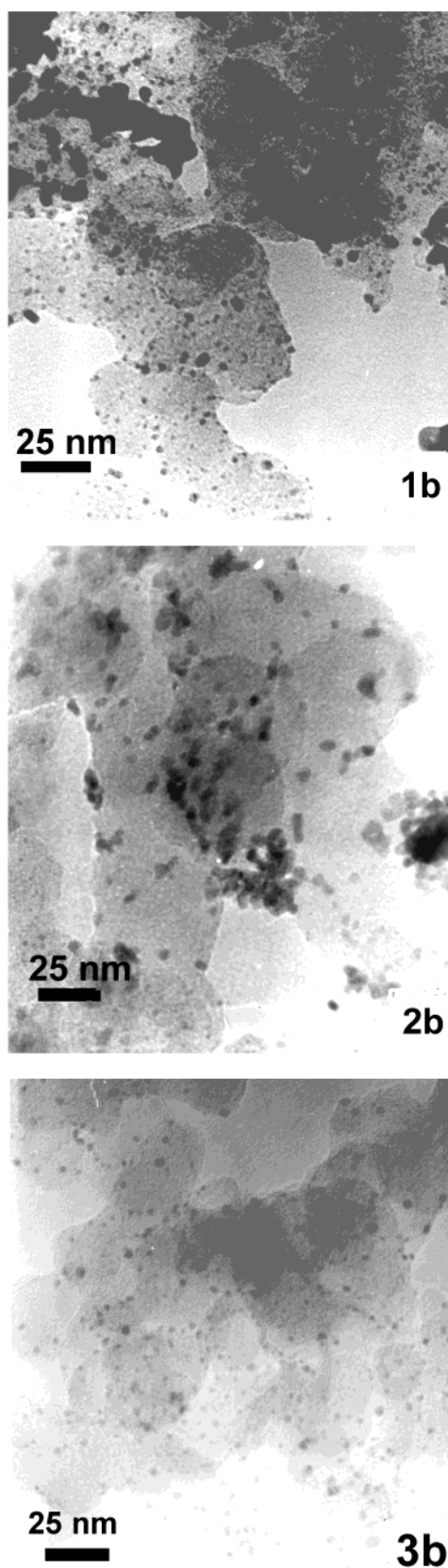


**Figure 1.** Bright-field TEM micrograph typical of the Os/Vulcan carbon nanocomposites **1b** and **2b** and the Pt–Os/Vulcan carbon nanocomposite **3b**.

nation of volume-weighted Os nanocluster average diameter from XRD peak widths through application of Scherrer's equation gives Os particle sizes of  $4.0 \pm 1.2$  nm and  $7.0 \pm 1.5$  nm, respectively. For nanocomposite

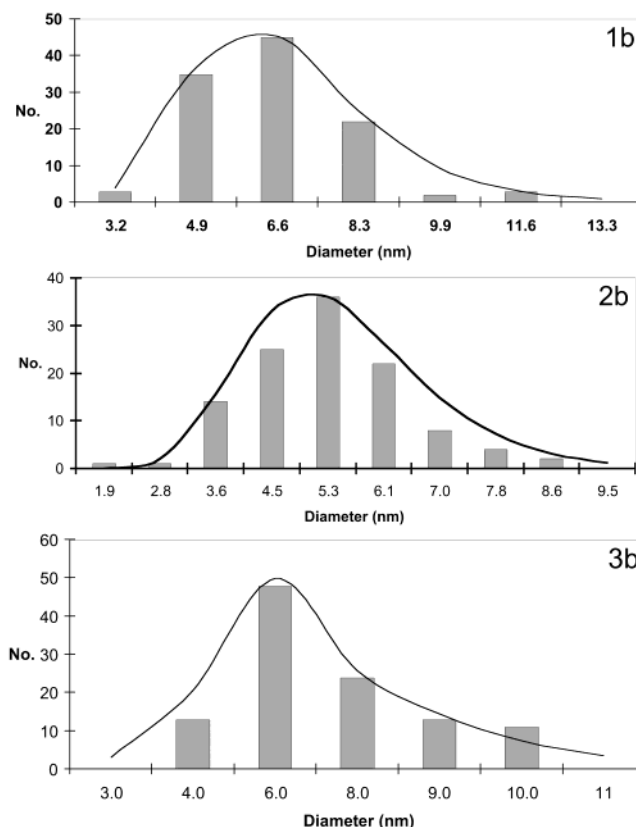


**Figure 2.** Histograms of metal nanocluster diameters typical of the Os/Vulcan carbon nanocomposites **1b** and **2b** and the Pt–Os/Vulcan carbon nanocomposite **3b** as measured from TEM micrographs.

**3b**, all of the remaining peaks have positions and relative intensities expected for diffraction from a single-phase fcc Pt–Os alloy having a cell constant of  $3.889 \pm 0.013$  Å. Assuming that arc-melted Pt–Os alloys have lattice constant-compositional dependency that follows Vegard's law behavior, a 1:1 Pt–Os alloy should have a lattice constant of ca. 3.888 Å.<sup>2b</sup> A determination of volume-weighted Pt–Os nanocluster average diameter from XRD peak widths through application of Scherrer's equation gives an average particle size of  $9.2 \pm 1.3$  nm. Close correspondence between metal particle sizes determined from XRD data and TEM measurements indicates the absence of significant numbers of atypically large metal nanoclusters within the sample.

Nanocomposites **1b–3b** have been evaluated as methanol electrooxidation catalysts both electrochemically and in working DMFCs. A sample of nanocomposite **2b** was incorporated into a single, 25 cm<sup>2</sup> membrane electrode assembly (MEA) at a metal loading of 2.7 mg Os/cm<sup>2</sup> of electrode surface. Two MEAs were prepared of nanocomposite **3b** having an area 25 cm<sup>2</sup> and a total metal loading of 1.5 mg/cm<sup>2</sup>. DMFCs fabricated with these MEAs using Pt black (4 mg Pt/cm<sup>2</sup>) as a cathode were tested under standard operating conditions.<sup>5c</sup> At open circuit, DMFC cell potentials were 0.520 V for the Os/carbon nanocomposite and 0.60 V for the Pt–Os/carbon nanocomposite. However, cell voltage dropped dramatically (to less than 0.20 or 0.30 V, respectively) upon application of low current loads (0.05 A/cm<sup>2</sup> and 0.20 A/cm<sup>2</sup>, respectively) and decreased to less than 0.10 V with sustained or modest current load. Upon removal of the current load, cell potential increased to the

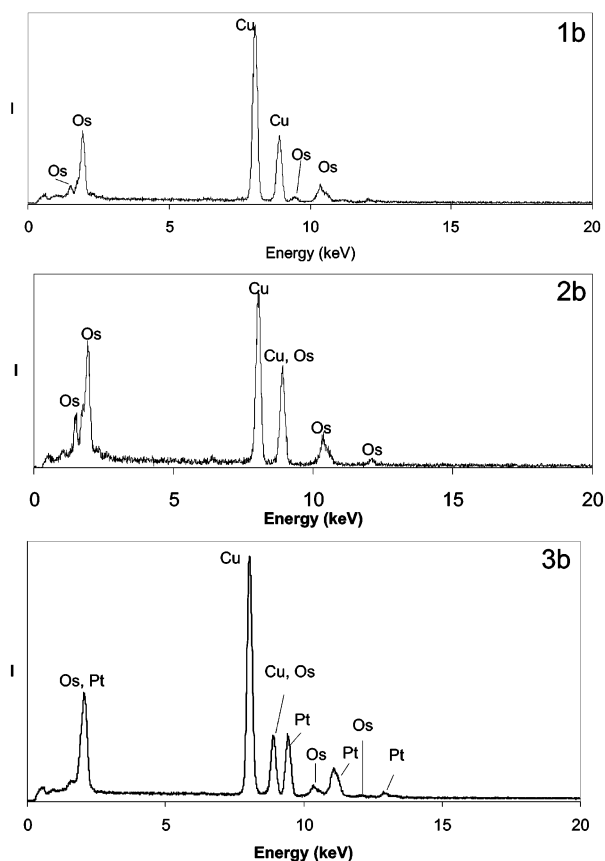


**Figure 3.** Broad-area EDS spectra typical of the Os/Vulcan carbon nanocomposites **1b** and **2b** and the Pt–Os/Vulcan carbon nanocomposite **3b**. Emission from Cu present within the sample holder is also observed.

original open-circuit value. These results indicate that although Os and Pt–Os alloy nanoparticles are thermodynamically capable of oxidizing methanol, the dramatic drop in cell potential with applied load indicates poor kinetic turnover for this reaction.

Because DMFC performance deteriorates too rapidly to obtain acceptable  $i$ – $V$  curves, nanocomposites **1b**–**3b** were examined as methanol electrooxidation catalysts using an electrochemical cell designed for combinatorial fuel cell measurements.<sup>12</sup> Discharge performance  $i$ – $V$  curves for a cell fabricated with **1b**, **2b**, Pt black, a 2:1 mixture of **1b** and Pt black, a 2:1 mixture of **2b** and Pt black, nanocomposite **3b**, and commercial, unsupported 1:1 Pt–Ru alloy colloid, as methanol electrooxidation catalysts are shown in Figure 5.

The performance of nanocomposites **1b** and **2b** is significantly less than that recorded for any of the other anode catalysts examined. Open-circuit potentials for nanocomposites **1b** and **2b** are in the range 0.2–0.3 V with electrode potential dropping rapidly with applied current load. Electrode potentials fell below 0.10 V with current loads of less than 0.05 mA. This rapid decline in electrode potential upon application of a load parallels the rapid drop in performance observed for these nanocomposites as DMFC anode electrocatalysts. Admixture of Pt black cocatalyst with nanocomposites **1b** and **2b** leads to improved performance. Open circuit potentials rise to 0.4–0.5 V with cell potentials decreasing to below 0.10 V at current loading as high as 0.28–0.35 mA. The performance of both of these Os/Pt/carbon binary metal

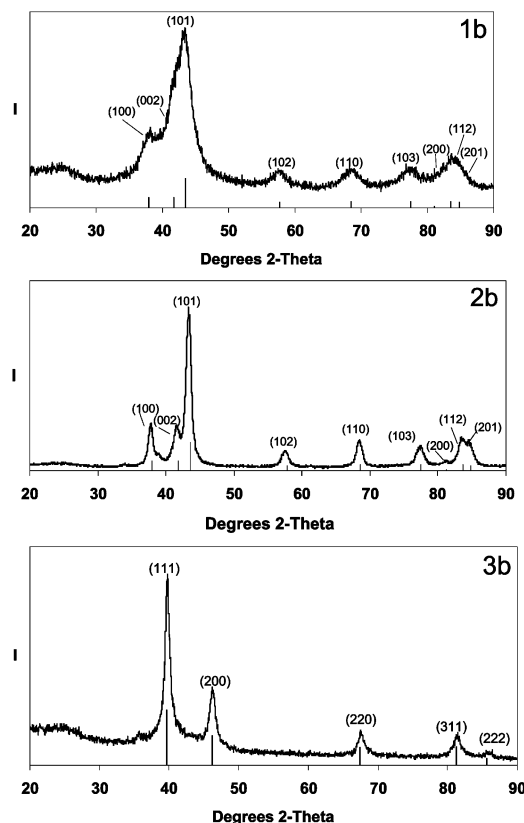


**Figure 4.** Powder XRD patterns typical of the Os/Vulcan carbon nanocomposites **1b** and **2b** and the Pt–Os/Vulcan carbon nanocomposite **3b**, including the standard line pattern and peak assignments for Os metal or for fcc Pt metal.

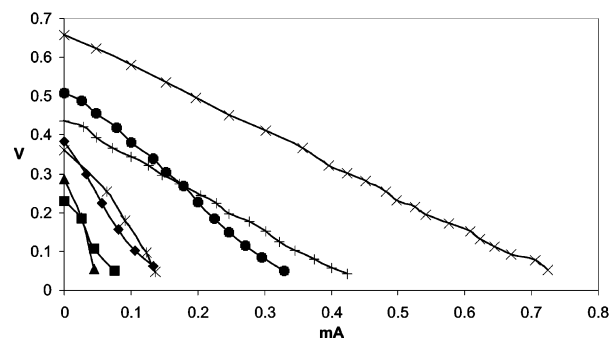


**Figure 5.** Discharge polarization current density–voltage (V) curves recorded for methanol oxidation using a proprietary combinatorial fuel cell anode (electrode area = 0.03 cm<sup>2</sup>) spotted with nanocomposite **1b** (■), nanocomposite **2b** (▲), Pt black (◆), a 2:1 mixture of nanocomposite **1b** and Pt black (●), a 2:1 mixture of nanocomposite **2b** and Pt black (+), nanocomposite **3b** (\*), and a commercial, unsupported 1:1 Pt–Ru alloy colloid (x), as electrooxidation catalysts.

composites exceeds the performance recorded when Pt black is used as the anode electrocatalyst.

The performance of nanocomposite **3b** is better than that of nanocomposites **1b** and **2b** and comparable to the performance of Pt black. The open-circuit potential observed for nanocomposite **3b** is 0.36 V, with electrode potential dropping rapidly with applied current load. This rapid decline in electrode potential upon application of a load parallels the rapid drop in performance observed for this nanocomposite as a DMFC anode electrocatalyst. All of the electrocatalysts examined in this study perform well below the performance recorded of the 1:1 Pt–Ru unsupported electrocatalyst, which is

a commonly used standard for evaluating relative catalytic performance for methanol electrooxidation. It is important to note that the relative performances of electrocatalysts examined in this study are obtained from samples as-prepared or as obtained. No attempt has been made to correct catalyst performances for differences in metal surface area or in the number density of reactive surface sites.

### Conclusions

Os and Pt–Os/carbon nanocomposites have been prepared using three complexes as single-source precursors of metal. Thermal decomposition of precursor/carbon composites under solely reducing conditions gives metal/carbon nanocomposites of high metal loading. Metal nanocrystals of ca. 5–7 nm average diameter (by TEM) are observed highly dispersed on a Vulcan carbon powder support. DMFC and electrochemical measurements reveal thermodynamically favorable but kinetically slow electrooxidation of methanol by either the Os metal or Pt–Os alloy/carbon nanocomposites.

Admixture of Pt black colloid with these Os/carbon nanocomposites gives methanol oxidation catalysts of improved performance; however, these phase-separated binary metal composite catalysts still perform poorly relative to a 1:1 Pt–Ru colloidal electrocatalyst. Although the predicted reactivity of nanocrystalline Os as a methanol electrooxidation catalyst has been demonstrated using the Os nanocomposites prepared in this study, the rate of this reaction is too slow to be of practical importance.

**Acknowledgment.** Research support provided by the U.S. Army Research Office under grants DAAH04-95-1-0146, DAAH04-96-1-0179, DAAH04-96-1-0302, and DAAG55-98-1-0362 is gratefully acknowledged by C.M.L. Support from MURI Contract DA/DAAH04-95-1-0094 is gratefully acknowledged by G.A.D. D.C. and R.J. acknowledge support received through the U.S. Army Research Laboratory Director's Research Initiative Program. We also thank Dr. D. A. Shores for helpful discussions.

CM011565C